Kao, W. W.-Y., Prockop, D. J., & Berg, R. A. (1979) *J. Biol. Chem. 254*, 2234.
King, J., & Laemmli, U. K. (1971) *J. Mol. Biol. 61*, 465.
Kivirikko, K. I., Kishida, Y., Sakakibara, S., & Prockop, D. J. (1972) *Biochim. Biophys. Acta 271*, 347.
Lazarides, E., Lukens, L. N., & Infante, A. A. (1971) *J. Mol. Biol. 58*, 831.
McGee, J. O'D., Jimenez, M. H., Felix, A. M., Cardinale, G. J., & Udenfriend, S. (1973) *Arch. Biochem. Biophys. 154*, 483.
Miller, E. J. (1971) *Biochemistry 10*, 3030.
Miller, E. J. (1972) *Biochemistry 11*, 4903.
Miller, E. J., Woodall, D. L., & Vail, M. S. (1973) *J. Biol. Chem. 248*, 166.
Okada, K., Kikuchi, Y., Kawashiri, Y., & Hiramoto, M. (1972) *FEBS Lett. 28*, 226.
Peterkofsky, B., & Udenfriend, S. (1963) *J. Biol. Chem. 238*, 3966.
Peterkofsky, B., & Assad, R. (1976) *J. Biol. Chem. 251*, 4770.
Prockop, D. J., Berg, R. A., Kivirikko, K. I., & Uitto, J. (1976) in *Biochemistry of Collagen* (Ramachandran, G. N., & Reddi, A. H., Eds.) p 163, Academic Press, New York.
Prockop, D. J., Kivirikko, K. I., Tuderman, L., & Guzman, N. A. (1979) *N. Engl. J. Med. 301*, 13, 17.
Uitto, J., & Prockop, D. J. (1974a) *Arch. Biochem. Biophys. 161*, 210.
Uitto, J., & Prockop, D. J. (1974b) *Biochim. Biophys. Acta 336*, 234.

Metal Ion Binding to α-Lactalbumin Species†

Kentaro Murakami,‡ Piet Jan Andree,§ and Lawrence J. Berliner*,‖

ABSTRACT: A strong cation (calcium) binding site has been demonstrated to exist in several α-lactalbumin species: bovine, goat, human, and guinea pig. A metal ion induced conformational change occurs, resulting in a unique (10–14-nm) blue shift and relative quenching of Trp fluorescence for all species. Calcium ion binding to the α-lactalbumins yielded dissociation constants (K_{diss} consistently in the 10^{-10}–10^{-12} M range, while Mn(II) binding was in the 20–30 μM range. Independent determinations of these cation binding equilibria were made by ESR measurements of free unliganded Mn(II) in titrations with the bovine species. One strong site (K_{diss} = 30.5 μM) was found, which correlated directly with the fluorescence-associated cation binding, plus three weaker sites (K_{diss} = 1.1, 5.0, and 5.0 mM, respectively). Several lanthanides as well as Mg(II) were found to displace Mn(II) from the strong site on bovine α-lactalbumin (as monitored by ESR) and to cause the identical fluorescence changes as found for Ca(II) and Mn(II) above. The importance of measuring these equilibria by both fluorescence and ESR was borne out by demonstrating the potential errors in estimating dissociation equilibria by the fluorescence method alone. Also, the errors in estimating K_{diss} for samples containing partially metal bound apo-α-lactalbumin are described as well as rapid, sensitive methods for estimating the extent of metal-free protein and correctly accounting for residual bound metal in equilibrium calculations.

α-Lactalbumin (αLA)[1] serves as a "modifier" protein in lactose biosynthesis ("lactose synthase") as the noncatalytic subunit in complex with galactosyltransferase (UDP-galactose:D-glucose 4-β-D-galactosyltransferase, EC 2.4.1.22). The metal binding properties of bovine αLA (BLA) were discovered in our laboratory by ESR and NMR as part of control experiments for Mn(II) binding to the catalytic subunit of the lactose synthase complex (Berliner et al., 1978; Andree & Berliner, 1980). Both Brittain et al. (1976) and Hiraoka et al. (1980) presented evidence for Tb(III) and Ca(II) binding to bovine αLA, respectively, but no equilibrium data were presented nor specific evidence for the exact binding locus. Precise determination of cation–αLA equilibrium binding constants and stoichiometry [for, e.g., Mn(II), Tb(III), etc.] is crucial to NMR, ESR, and fluorescence measurements of intermolecular distance relationships in the physiologically significant lactose synthase complex.

We have also been involved in characterization of structural homologies in a series of αLA species (Berliner & Kaptein, 1981) and have addressed whether these metal ion binding phenomena are common to most α-lactalbumins as a general structural feature. We present fluorescence and ESR measurements of the binding equilibria for several cations [Ca(II), Mn(II), Cd(II), Mg(II), lanthanides] with bovine, goat, human, and guinea pig α-lactalbumins. A subsequent paper will describe NMR evidence for the specific amino acid residue(s) affected by this cation binding, in particular that region adjacent to histidine-68 in bovine and goat α-lactalbumins (H. Nishikawa, K. Murakami, and L. J. Berliner, unpublished experiments).

Experimental Procedures

Proteins. Electrophoretically pure bovine αLA (lots 75C 8110, 86C 8020, and 50F 8105) was from Sigma Chemical Co. Other αLA species were obtained or isolated as noted

† From the Department of Chemistry, The Ohio State University, Columbus, Ohio 43210. *Received May 26, 1982.* Supported in part by grants from the National Institutes of Health (GM 21923) and the National Science Foundation (PCM 77-24658). A preliminary report on part of these results was published earlier (Berliner et al., 1978). Some of this work was also presented at the IVth International EPR Symposium, 23rd Rocky Mountain Conference, Denver, CO, Aug 1981.

‡ Recipient of an Ohio State University postdoctoral fellowship, 1979–1980.
§ Recipient of an Ohio State University postdoctoral fellowship, 1976–1977. Present address: Duphar BV, Weesp, The Netherlands.
‖ Established Investigator of The American Heart Association.

[1] Abbreviations: αLA, α-lactalbumin; BLA, bovine α-lactalbumin; GLA, goat α-lactalbumin; HLA, human α-lactalbumin; GPLA, guinea pig α-lactalbumin; ESR, electron spin resonance; EDTA, ethylenediaminetetraacetic acid; EGTA, ethylene glycol bis(β-aminoethyl ether)-*N*,*N*,*N*′,*N*′-tetraacetic acid.

0006-2960/82/0421-5488$01.25/0

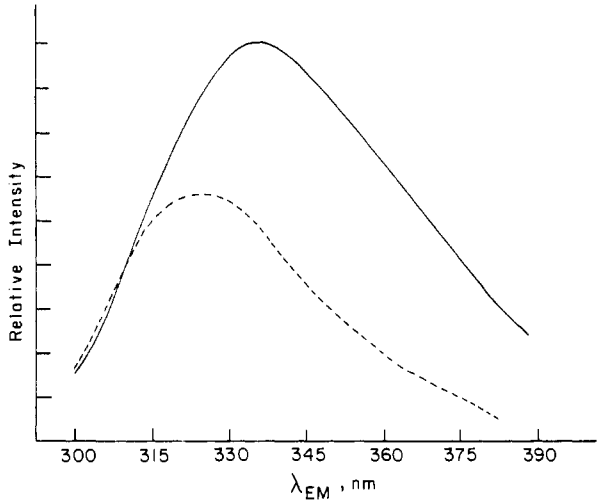

FIGURE 1: Intrinsic fluorescence spectra of bovine αLA at pH 7.4 (0.05 Tris-HCl, 26 ± 0.5 °C). The solid line is apo-bovine αLA. The dashed spectrum is Ca(II)-saturated protein. The excitation wavelength was 280 nm. (While identical spectral line shapes were observed over the excitation wavelength range 280–295 nm, it was experimentally preferable to use a 280-nm excitation to reduce any light-scattering problems in the emission spectra on this instrument.)

earlier (Berliner & Kaptein, 1981). Bovine αLA preparations that contained partially bound Ca(II) were demetallized by the procedure discussed below.

Chemicals. Ultrapure manganese chloride (99.999%, lot 0518), cadmium chloride (99.999%, lot 0818), and zinc chloride (99.999%, lot 0208) were from Aldrich Chemical Co. EGTA (97–98%, lot 80F-5048) was from Sigma Chemical Co. EDTA (99+%, lot 011581) was from Alfa Products. Lanthanide compounds were purchased as the chlorides of the highest grade purity from either Alfa Products (99.9%) or Aldrich Chemical Co. (99.99%). Ultrapure ammonium sulfate (lot BZ-2740) was purchased from Schwarz/Mann.

Methods. (*A*) *Fluorescence measurements* were made on a Perkin-Elmer MPF-44A spectrofluorometer with a thermostated cell compartment (26 ± 0.5 °C).

(*B*) *ESR experiments* were carried out on a Varian E-4 as "titrations" of free uncomplexed Mn(II) in capillary cells as described earlier (Andree & Berliner, 1980). Each spectrum was followed by a standard Mn(II) solution (pH 7.4, 0.05 M Tris-HCl) taken under the same conditions to correct for slight changes in instrumental response. Where $Mn(II)_{free}$ concentrations were quite low (<10 μM), the spectra were averaged and the base line was corrected on a Varian E-935 data system. Atomic absorption measurements for Ca(II) were made on Perkin-Elmer Models 303 or 360. Proton water T_1 measurements were made on Bruker HX90, WP80, and BKR 322S instruments.

(*C*) *Demetallization* of the Sigma α-lactalbumin preparation was required as the lots typically contained up to 23% calcium/mol by atomic absorption. The procedures outlined below were most effective for maximum calcium removal without any residual EDTA or EGTA chelating agent remaining in the final purified sample (as checked by ^1H NMR). A 4 mg/mL αLA sample in 100 mM EDTA (0.05 M Tris-HCl, pH 7.4) at room temperature was precipitated after 30 min with 95% ultrapure $(NH_4)_2SO_4$. This step was then repeated except with 100 mM EGTA, then 95% $(NH_4)_2SO_4$ precipitation was done, and finally a single chromatographic step on Bio-Gel P-2 (0.05 M Tris-HCl, pH 7.4) was performed to remove residual salts. We found that dialysis as an alternative to the steps above resulted in significant residual concentrations of chelating agent remaining over several days.[2] If exhaustive dialysis of apo-αLA was utilized in place of the Bio-Gel P-2 step, an eventual remetallization of the apoprotein occurred even with demineralized doubly or triply distilled water that had been treated with Chelex 100 prior to use. All glassware, etc., were first acid–EDTA washed and then rinsed with Chelex 100 treated water several times. Typically, our bovine αLA preparations were 95–99% metal free by atomic absorbance and fluorescence (see Results).

Data Analysis. Fluorescence titrations were fit to a single hyperbolic isotherm using a nonlinear regression scheme (Marquardt's algorithm) on a Hewlett-Packard 9835 calculator. Bound metal ion was calculated from a fluorescence quenching factor

$$R = q_{obsd}^{360nm}/q_{max}^{360nm} \quad (1)$$

where

$$q_{obsd}^{360nm} = 1 - \frac{\text{observed } \alpha\text{LA intensity (360 nm)}}{\text{apo-}\alpha\text{LA intensity (360 nm)}} \quad (2)$$

$$q_{max}^{360nm} = 1 - \frac{\text{metal-saturated } \alpha\text{LA intensity (360 nm)}}{\text{apo-}\alpha\text{LA intensity (360 nm)}} \quad (3)$$

and

$$[\text{metal}]_{free} = [\text{metal}]_{total} - R[\alpha\text{LA}]_{total} \quad (4)$$

This analysis assumed a cation stoichiometry of 1:1, which, while strictly not correct, altered the fluorescence determined dissociation constants by 1 or 2% (see Discussion). In every experiment the apo-αLA intensity was checked by adding small aliquots of EGTA until the intensity at 360 nm and the λ_{em}^{max} did not increase further.[3]

ESR-determined equilibrium constants were based on direct measurement of free Mn(II), as described earlier (Berliner & Wong, 1975; Andree & Berliner, 1980), where the fraction of bound manganese to total protein is

$$\mu_{obsd} = (1 - \theta)[\text{Mn}]_{total}/[\alpha\text{LA}]_{total} \quad (5)$$

where we have defined

$$\theta = [\text{Mn}]_{free}/[\text{Mn}]_{total} \quad (6)$$

as the fraction of free to total Mn(II).

These data were fit by nonlinear regression to a multiparameter Scatchard plot.

Competitive binding experiments were made by either EGTA fluorescence "back-titrations" of Ca(II)-bound αLA species or ESR competitive displacement titrations of fixed Mn(II)–αLA complexes. Dissociation equilibria were calculated on the basis of known Ca(II)–EGTA or Mn(II)–αLA equilibrium constants.

Results

Fluorescence Measurements. The intrinsic fluorescence emission spectra of all αLA species examined in this study were both partially quenched and blue shifted upon titration with

[2] If a 1-mL sample of ca. 5 μM apo-bovine αLA sample were dialyzed over a 24-h period vs. 0.5–1 L of doubly distilled demineralized Chelex 100 treated water or Tris buffer, sufficient trace metal impurity [Ca(II)?] was absorbed by the protein as evidenced by changes in its fluorescence parameters (I_{360}/I_{max}) and its insensitivity to exogenously added Ca(II) (see Figures 1 and 2).

[3] The ratio R was valid for any wavelength; however, the intensity at 360 nm (I_{360}) was the most sensitive part of the emission curve to metal binding.

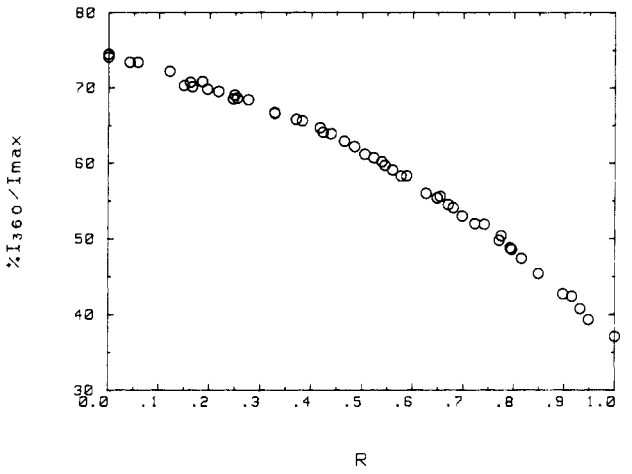

FIGURE 2: Fluorescence calibration curve for bovine α-lactalbumin of percent I_{360}/I_{max} vs. $R = q_{obsd}/q_{max}$. The parameters were measured from the intrinsic fluorescence emission spectrum (λ_{ex} = 280 nm) of a 5 μM bovine αLA solution (0.05 M Tris-HCl, pH 7.4, 26 ± 0.5 °C) by either (a) a Ca(II) titration of apo-bovine αLA [of precisely known trace Ca(II) content by atomic absorbance] or (b) an EGTA back-titration of Ca(II)–αLA (1:1). There was also a concomitant blue shift in λ_{max}^{em} with increasing R (see Figure 1). Exactly the same fluorescence behavior was observed with Mn(II) and Cd(II) as well as several lanthanide cations. The percent I_{360}/I_{max} ratio serves as the most sensitive indicator of the fraction of bound cation [especially Ca(II) impurities] that is directly related to the parameter R. Similar calibration curves were prepared for the other αLA species. The curve for goat αLA was essentially identical with that for bovine αLA, while GPLA and HLA differed slightly, due to their altered Trp content.

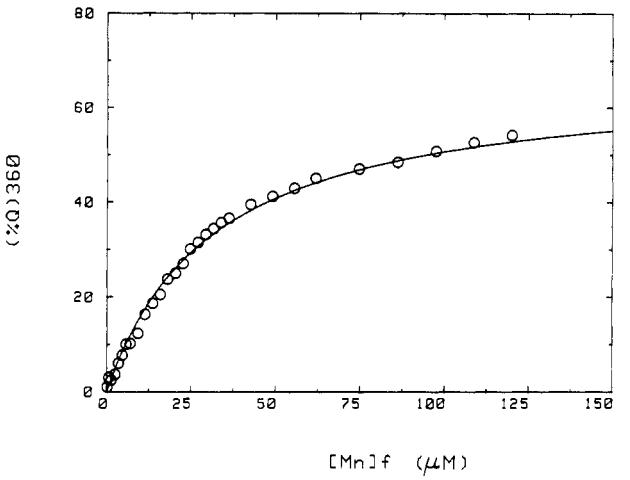

FIGURE 3: Fluorescence titration of apo-bovine αLA with $MnCl_2$, pH 7.4, and 0.05 M Tris-HCl; $[\alpha LA]_{total}$ = 5.6 μM. The solid line is the theoretical fit to K_{diss} = 31.7 μM. All other parameters were as in Figure 1 or 2.

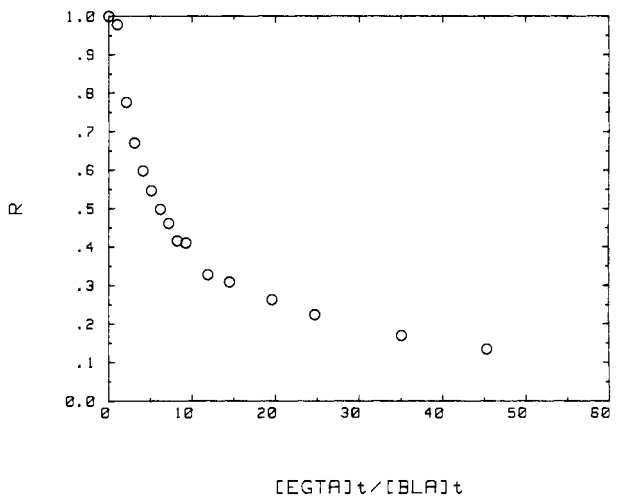

FIGURE 4: Fluorescence titration of Ca(II)–bovine α-lactalbumin (1:1) with EGTA. All other conditions were as in Figure 1 or 2. The data were subsequently fit to a linearized form of a competitive binding model that optimized the function $(1 - R)/R$ vs. S, where $S = [EGTA]_{total}/([Ca(II)]_{total} - R[\alpha LA]_{total})$. The K_{diss} for several determinations was 2×10^{-10} M.

several cations [e.g., Ca(II) and Mn(II)]. Figure 1 shows the fluorescence spectra of apo- and Ca(II)-saturated bovine αLA. The emission maximum shifts from 337.5 to 324.5 nm upon binding 1 mol of metal ion. A pronounced decrease ("quenching") of fluorescence intensity is monitored at 360 nm, which is directly proportional to the fraction (R) of metal bound to a single high-affinity site. It is critical, however, to know *precisely* the fraction of bound cation in the initial "apo" protein sample; otherwise, q_{obsd}^{360nm} (eq 2) is overestimated, R (eq 1) is overestimated, and consequently $[metal]_{free}$ (eq 4) and thus K_{diss} are underestimated. The magnitude of the underestimate in $[metal]_{free}$ is directly related to the total protein concentration, $[\alpha LA]_{total}$ (eq 4). Figure 2 depicts the change in the ratio of the emission intensity at 360 nm to the intensity at the emission maximum wavelength, percent I_{360}/I_{max}, for αLA that is complexed with Ca(II) at varying levels of substitution. The value R is directly related to the mole fraction of bound cation. The I_{360}/I_{max} ratio turns out to be the most sensitive parameter that can be measured directly from the fluorescence spectra and is not dependent on the concentration reproducibility characteristics of the spectrofluorometer. Furthermore, apoprotein samples that contain residual Ca(II) may be corrected for this initially bound metal in a subsequent titration by a correction procedure that yields the correct K_{diss} (see the Appendix).

The binding of $MnCl_2$ to apo-bovine αLA was also shown by fluorescence to induce precisely the same changes in emission and intensity parameters as was found with Ca(II). The data shown in Figure 3 were fit by nonlinear regression analysis to a K_{diss} = 31.7 ± 1.4 μM. The binding of Ca(II) and several lanthanides was, on the other hand, extremely strong. In the case of Ca(II) a "direct metal titration" by fluorescence was not at all accurate since the K_{diss} was several orders of magnitude smaller than the lowest observable protein concentrations. Almost any method of "direct" analysis, including equilibrium dialysis, would suffer the same experimental inaccuracy. Therefore, a competitive back-titration with EGTA was carried out at pH 7.4 by using the known binary dissociation constant for Ca(II)–EGTA of 8.5×10^{-10} M at this pH (Kim & Padilla, 1978). The data are shown in Figure 4 for bovine αLA from which was calculated a Ca(II)–BLA dissociation constant, $K_{diss} = 2.3 \times 10^{-10}$ M, which was 1 order of magnitude stronger than that reported by Permyakov et al. (1981a) at pH 8.04. We also found evidence for several other metals that bound to BLA, including several lanthanides [Tb(III), Eu(III), Gd(III), Yb(III), Pr(III), Dy(III), Cd(II), Mg(II), Co(II), and Zn(II)]. The binding of Co(II) and Zn(II), however, did not follow the same fluorescence changes as for other metals (see Figure 2) but rather they bound at a secondary site or sites, which will be reported later. Our results for this series of cations, which were found to bind to bovine αLA, are compiled in Table I. In all cases with the exception of Co(II) and Zn(II) the emission wavelength and line shape changes were identical regardless of the cation employed. All of the lanthanides bound with dissociation constants comparable to that of Ca(II), i.e., ca. 10^{-10} M, but were not quantitated precisely due to a lack of accurate dissociation constants for lanthanide–EGTA or

Table I: Bovine αLA Metal Ion Equilibria[a]

cation	K_{diss} determined by fluorescence	ESR
Ca(II)	2×10^{-10} M	too small to estimate[b]
Mn(II)	31.7 μM	30.5 μM, 1.1 mM, 5.0 mM, 5.0 mM
Cd(II)	2.5 μM	
Mg(II)	0.67 mM[c]	0.75 mM
Tb(III), Dy(III), Yb(III), Gd(III), Eu(III)	$\sim 10^{-10}$–10^{-12} M[d]	too small to estimate[b]

[a] pH 7.4, 0.05 M Tris-HCl, 26 °C. [b] A stoichiometric release of $Mn(II)_{free}$ was observed per aliquot of cation titrated (see Figure 6). [c] Compare with the values of 0.5 mM and 5 mM for a strong and weak site, respectively, reported by Permyakov et al. (1981b). [d] The K_{diss} could not be accurately determined from a direct Ca(II) titration since the lower limit of protein concentration was larger than 1.0 μM. An EGTA competitive back-titration could not be evaluated without the individual equilibrium constants for each lanthanide. The evidence above as well as that from NMR observations suggests that these cations bind to the same Ca(II) site with comparable affinities.

Table II: Fluorescence Parameters and Associated Equilibria for Apo- and Metal-Bound α-Lactalbumin Species[a]

species	bovine (BLA)	goat (GLA)	human (HLA)	guinea pig (GPLA)
apo-αLA				
λ^{em}_{max} (nm)	338	338	338	332
$\%\, I_{360}/I_{max}$	74.5	74.1	70.0	58.0
Ca(II)–αLA				
λ^{em}_{max} (nm)	324	324	327	323
$\%\, I_{360}/I_{max}$	37.1	32.8	45.1	30.0
$\%\, q$	71.1	71.2	59.8	64.7
K_{diss}				
Ca(II) (nM)	0.2		0.03	0.005
Mn(II) (μM)	31.7	17.0	26.9	
Mn(II), ESR	30.5 μM, 1.1 mM, 5.0 mM, 5.0 mM			

[a] pH 7.4, 0.05 M Tris-HCl, 26 °C. The fluorescence parameters I_{360}/I_{max} and q are described under Experimental Procedures.

EDTA. Some relative competitive binding equilibria between Ca(II) and some of the lanthanide shift reagents were estimated from proton NMR studies (H. Nishikawa, K. Murakami, and L. J. Berliner, unpublished results).

Cation Binding to Other α-Lactalbumin Species. Our findings that Ca(II) and Mn(II) bound to several other α-lactalbumin species were strongly suggestive of a homologous sequence (conformational) segment in these immunologically and physiologically cross-reactive forms (Ley & Jenness, 1970; Prieels et al., 1979). A detailed characterization of their surface residues has been reported earlier and has already found remarkable homology (Berliner & Kaptein, 1981). Table II summarizes our results with bovine, goat, human, and guinea pig α-lactalbumins. The fluorescence emission spectral parameters are slightly different from one another, particularly HLA and GPLA, which lack a specific Trp fluorophore (Sommers & Kronman, 1980). Yet despite a few nanometer differences in their λ^{em}_{max} values, all display a significant blue shift upon cation binding. The Ca(II) dissociation constants are quite strong and within 1 order of magnitude of each other. Where we were not sample limited, we were able to demetallize the protein and measure the Mn(II) binding equilibria as well (see Table II). In order to quickly analyze a new sample for the extent of residual bound metal before attempting a cation binding experiment, we prepared calibration curves similar to

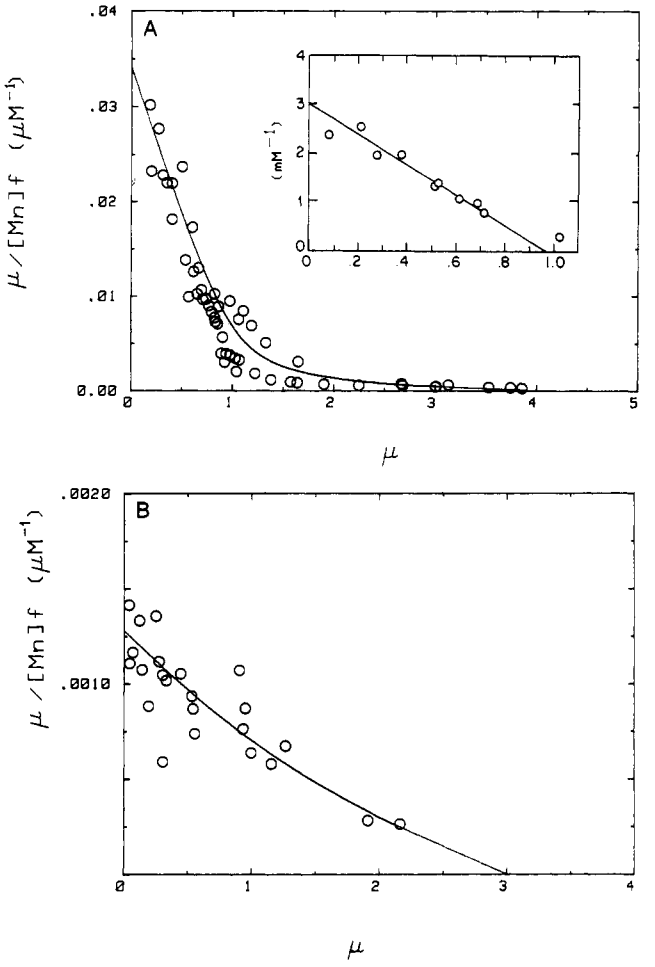

FIGURE 5: Scatchard plot of ESR titrations of bovine α-lactalbumin with Mn(II), pH 7.4 (0.05 M Tris-HCl, 26 ± 2 °C). (A) Apo-αLA. The solid line is a best fit multisite analysis for four sites of K_{diss} = 30.5 μM, 1.1 mM, 5.0 mM, and 5.0 mM. (Inset) Apo-αLA in the presence of 0.1 M $(NH_4)_2SO_4$. The solid line is best fit to a single site of K_{diss} = 300 μM. (B) Ca(II)-*loaded* apo-αLA (1:1). Here the strong site corresponding to K_{diss} = 30.5 μM in (A) above is blocked with Ca(II). The remaining weaker sites were fit to K_{diss} = 1.1, 5.0, and 5.0 μM, respectively. The Ca(II)-loaded protein was prepared by adding a slight molar excess of $CaCl_2$ to the apoprotein followed by dialysis.

that in Figure 2 for each species.

ESR Binding Measurements of Mn(II) and Other Cations. The binding of Mn(II) may be measured directly by the decrease in the free Mn(II) spectrum upon complexation since the complexed Mn(II) spectrum is broadened to such an extent that its spectral contribution is negligible under the conditions used to attain the range of binding stoichiometry needed for an accurate equilibrium measurement. Figure 5A shows a Scatchard plot of Mn(II) binding to apo-BLA. The data are consistent with a single strong binding site and three weaker sites. In order to obtain a quantitative measure of the contributions of the weak sites to the overall binding, we prepared "Ca(II)-loaded" BLA that contained exactly equimolar Ca(II) and protein by atomic absorption. Figure 5B depicts a Scatchard plot for the binding of Mn(II) to sites 2–4. The Ca(II) binding affinity to site 1 is so strong (as noted in Tables I and II) that no competition for this site by Mn(II) occurs over the concentration ranges employed in Figure 5. The effects of increased ionic strength are shown in the inset to Figure 5A, where only a single strong site of K_{diss} = 300 μM was accurately measurable in 0.1 M $(NH_4)_2SO_4$. The dissociation constants calculated for each site in Figure 5 are summarized in Table I. The excellent agreement between the

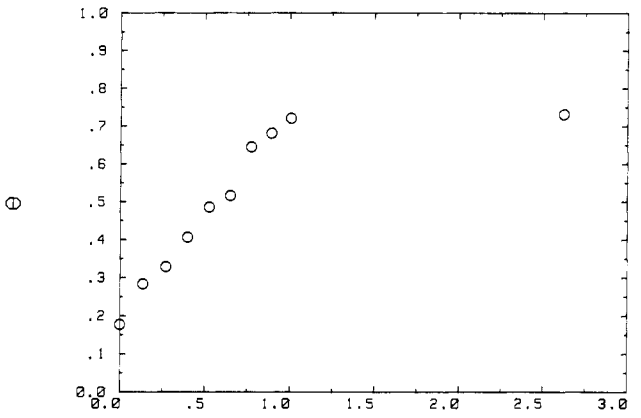

FIGURE 6: Ca(II) displacement of Mn(II) from bovine αLA. A fixed Mn(II)–BLA complex (0.4 mM:0.4 mM) was titrated with Ca(II) and plotted as the ratio of $[Ca(II)]_{total}$ to $[\alpha LA]_{total}$ vs. the fraction of Mn(II) that is free, $\theta = [Mn]_{free}/[Mn]_{total}$. Note that θ only very gradually rises above Ca(II) saturation of the strong cation site since weak site Mn(II) binding will occur to some extent under these conditions (see Figure 5). All other conditions are identical with those in Figure 5.

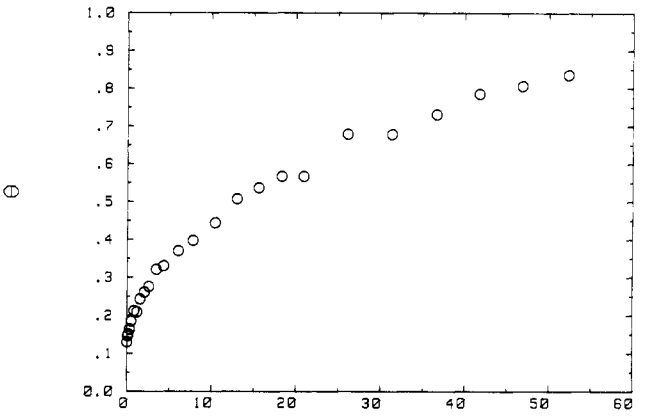

FIGURE 7: Displacement of Mn(II) from bovine αLA by Mg(II). The parameter θ is defined as in Figure 6. $[Mn(II)]_{total}$ = 0.39 mM; $[\alpha LA]_{total}$ = 1.0 mM. All other conditions are identical with those in Figure 5A.

K_{diss} for site 1 by ESR and that by fluorescence was only possible by using ultrapure $MnCl_2$.[4] If one corrects the fluorescence-calculated K_{diss} value for the three weak site(s) binding, the change in $Mn(II)_{free}$ concentration (eq 4) is manifested in at most a 1–2% change in the calculated K_{diss} [since at the Mn(II) concentrations employed in the fluorescence measurements the extent of weak site binding is quite small].

An apparent strong competition by Ca(II) for site 1 is demonstrated by ESR measurements in Figure 6 where we have plotted the net displacement of Mn(II) from the Mn(II)–BLA complex. Note the linear response to increasing Ca(II) to a 1:1 stoichiometry, which is reflective of a much stronger affinity of the protein for Ca(II) vs. Mn(II) and, as were the data in Figure 5B, consistent with competitive binding to the (strong) site 1.[5] Several lanthanides were titrated vs. Mn(II)–BLA by the same procedure to give identical results as that shown (Figure 6) for Ca(II), implying K_{diss} values of the same or stronger order (10^{-10}–10^{-11} M).[6,7] The binding of Mg(II) to BLA by Mn(II)-displacement ESR measurements is shown in Figure 7. The relative weak binding constant (vs. the other metals in Table I) was in quite good agreement with that obtained by fluorescence.

Further insight into the nature of the strong cation site may come from the water proton T_1^{-1} relaxation rate enhancement factor, ϵ_b. For Mn(II)–BLA under conditions where only site 1 (strong site) was occupied, we obtained an $\epsilon_b \approx 2.2$–2.5 over three different frequencies, 60, 80, and 90 MHz, respectively, which was unchanged in the presence or absence of 0.1 M $(NH_4)_2SO_4$. Addition of equimolar Ca(II) to the BLA sample shifted the observed enhancement factor close to that for free Mn(II).[8]

Discussion

The phenomenon of cation binding to αLA is common to several (and perhaps all) species particularly for Ca(II), a highly abundant cation in milk (Altman & Dittmer, 1971). The extremely "tight" dissociation constants measured for Ca(II) with each species (ca. 10^{-11} M) suggest that the physiological state of αLA should be the Ca(II)-bound form. The fluorescence spectral characteristics of these αLA species reflect distinct changes in Trp environments upon cation binding. The mechanism of the observed Trp emission and blue shift is not consistent with a direct contact quenching mechanism since Mn(II) and the lanthanides should be more effective quenching agents. Thus, the mechanism is more consistent with a ligand-induced conformational change, a suggestion already supported by the studies of Hiraoka et al. (1980) on the Ca(II)-induced stabilization of BLA to denaturation. Further evidence comes from our ^1H NMR studies of bovine αLA, which detects at least two distinct residue shifts that occur upon Ca(II) binding, as well as paramagnetic relaxation of one that results from Mn(II) binding (His-68) (H. Nishikawa, K. Murakami, and L. J. Berliner, unpublished experiments).

While the precise location of the cation site awaits further X-ray and NMR studies, the species similarities found here strongly suggest a common binding locus of highly conserved

[4] The importance of using ultrapure cation salts was quite evident with $MnCl_2$. When ACS reagent grade $MnCl_2$ (Fisher M-82, lot 751748), which contains 1–5 ppm of various heavy metals, was used, a K_{diss} for Mn(II)–BLA was measured as 1–2 μM. After dialysis of a fully titrated sample the fluorescence emission spectrum was that of fully metal liganded BLA (see Figure 1) reflecting the tight complexation of a heavy metal impurity, quite likely Ca(II). It is important to point out that the relatively high volumes and the relatively *low* number of total moles of protein favor a higher trace metal/protein ratio than do our ESR experiments.

[5] Direct evidence of competition for the same site comes from our ^1H NMR experiments to be published subsequently (H. Nishikawa, K. Murakami, and L. J. Berliner, unpublished results).

[6] When a protein sample contained initially bound Ca(II), the ESR titrations also yielded quite accurate measures of the extent of partially bound Ca(II) in experiments like that in Figure 6 where the curve leveled out at ratios of exogenously added metal to protein less than 1.0. In Scatchard plots like those in part A and the inset of Figure 5, the strong site portion of the curve extrapolated to values of $n < 1.0$. The agreement by atomic absorption analysis was remarkable.

[7] We have since measured secondary site Ca(II) binding to BLA by ESR under conditions similar to those in Figure 5B, where a K_{diss}(overall) = 0.40 ± 0.17 mM was obtained.

[8] If one compares this ϵ_b with that for proteins of similar size, and assuming fast exchange and τ_c = 2.6–5 ns, the calculated coordination number, q, is less than 1.0, suggesting inner sphere water ligand exchange is significantly restricted in the first coordination sphere (Dwek, 1973).

sequence homology throughout the αLA species. The strong preference for calcium-like ligands and the weaker binding with Mn(II) suggest that principally oxygen-containing ligands comprise the coordination moieties of this site. The Mn(II) water relaxation experiments are most consistent with a model comprising a high degree of protein coordination leaving at best one water proton in the first coordination sphere. The nature of the blue-shifted Trp residue(s) that is (are) conformationally linked to the cation site may be narrowed down by comparing the compositions of the αLA family described earlier (Table II). Of the four Trp residues in bovine and goat αLA one is replaced in human (residue 26) and guinea pig (residue 60), respectively. Of the remaining two Trp residues (104 and 118) the former has been shown by photo-CIDNP NMR to be directly solvent accessible in all of the αLA species studied here (Berliner & Kaptein, 1981) while the latter has been found to be buried by CIDNP and by conformational calculations on the bovine form (Warme et al., 1974). Since residue 104 was speculated to be intimately involved in an internal energy transfer quenching mechanism with Trp-26 and -60 (Sommers & Kronman, 1980), the similar fluorescence characteristics found for each species in Table II and the CIDNP results suggest that Trp-118 rather than Trp-104 is the principally affected fluorophore upon cation binding.

The ESR measurements of Mn(II) binding have allowed us to characterize more than one metal binding site and relate the fluorescence-sensitive binding to the strong cation site. That is, the excellent agreement between the Mn(II) binding curve as measured by fluorescence (K_{diss} = 31.7 μM) and the (strong) site 1 by ESR (K_{diss} = 30.5 μM) allows one to conclude that the blue-shifted Trp fluorescence is connected to a single strong metal site and is (apparently) insensitive to cation binding at the weak sites.[9]

The importance of studying physical phenomena by more than one method was clearly confirmed by our ability above to obtain essentially identical strong site dissociation constants for Mn(II)–BLA (Table I). Our initial attempts with reagent-grade $MnCl_2$ demonstrated both the extent of tight metal binding resulting from ppm levels of impurities in $MnCl_2$ and the significant underestimate in the magnitude of the calculated K_{diss}.[4] Knowledge of the existence and affinity of additional cation sites is critically important to future fluorescence and magnetic resonance based distance measurements. Since these methods are based essentially on dipolar type interactions with a 1/(distance)^6 dependence, an only slightly occupied secondary site may contribute significantly to such measurements if its distance from the fluorophore (or spin) in question is much closer than that of the principal (strong) site. Further consideration of multiple site binding becomes important in evaluation of dissociation equilibria such as that shown for the Mn(II)-induced fluorescence changes in Figure 3, where the observed physical change was correlated with a single equilibrium constant. Since evaluation of K_{diss} requires direct knowledge of the free ligand concentration, that fraction of total ligand bound to other (non-fluorescence-associated) sites would not be obtainable without the ESR-derived binding constants. While the correction for secondary site binding was relatively small in this case of Figure 3 and did not alter the K_{diss} here substantially, this is certainly not the case in general when binding stoichiometry is not known directly.

The appendix that follows describes how one may correctly estimate the K_{diss} for a fluorescence cation "titration" of an αLA sample containing residual partially bound Ca(II).

Acknowledgments

We are gratefully indebted to the following colleagues for advice and discussion: Dr. H. Nishikawa (Kyoto Prefectural University, Japan), Drs. H. Farrell and T. Kumosinski (U.S. Department of Agriculture, Philadelphia), and F. Prendergast (Mayo Foundation, Rochester, MN). We also thank Drs. T. Sweet and R. Mayer of this department for use of their atomic absorption instruments and Dr. H. Gilboa (Technion, Haifa, Israel) for assistance and use of the Bruker BKR 322S NMR.

Appendix

Correction Method for the Determination of K_{diss} for Cation Binding to a Partially Metal Bound Protein Sample. Since αLA has very strong affinity for, e.g., Ca(II), it is sometimes very difficult to prepare a completely pure apo-αLA sample, especially where one is sample limited. However, one can correctly estimate the K_{diss} value for another cation binding to this protein sample if the K_{diss} of the residual bound metal is at least 1 order of magnitude smaller than that of the cation titrant. First, the I_{360}/I_{max} ratio of the initial αLA sample (before titrating) was measured and R was calculated from the calibration curve, for example, for BLA (see Figure 2). Now, for example, in an Mn(II) titration of this sample, the observed fluorescence intensity at 360 nm, I_{360}^{obsd}, is the sum of three components

$$I_{360}^{obsd} = \mu_{apo}I_{apo} + \mu_{Ca}I_{Ca} + \mu_{Mn}I_{Mn} \quad (7)$$

where I_{apo}, I_{Ca}, and I_{Mn} are the fluorescence intensity at 360 nm of apo-, Ca(II)-saturated, and Mn(II)-saturated αLA, respectively, and μ_{apo}, μ_{Ca}, and μ_{Mn} are the fractions of total αLA that are metal free, Ca(II) bound, and Mn(II) bound, respectively. Since $I_{Ca} = I_{Mn} = I_{bd}$ and $\mu_{apo} + \mu_{Ca} + \mu_{Mn} = 1$, then

$$I_{360}^{obsd} = \mu_{apo}I_{apo} + I_{bd}(1 - \mu_{apo}) \quad (8)$$

$$\mu_{apo} = (I_{360}^{obsd} - I_{bd})/(I_{apo} - I_{bd}) \quad (9)$$

The value I_{bd} is determined from the intensity of the cation [or Ca(II)] saturated sample, while I_{apo} is determined by titrating an initial sample with EGTA until the intensity stops increasing.

During a titration

$$\mu_{Mn} = 1 - \mu_{Ca} - \mu_{apo} \quad (10)$$

and the term μ_{Ca} is a constant [since the Ca(II) binding is so strong] determined from the R parameter from the calibration curve (see Figure 2). The correct K_{diss} is found from a fit of $[Mn(II)]_{free}$ vs. μ_{Mn} over the range μ_{Mn} = 0 to $(1 - \mu_{Ca})$ where

$$[Mn(II)]_{free} = [Mn(II)]_{total}(1 - \mu_{Mn}) \quad (11)$$

References

Altman, P. L., & Dittmer, D. S. (1971) *Blood and Other Body Fluids*, pp 459–461, FASEB, Bethesda, MD.

Andree, P. J., & Berliner, L. J. (1980) *Biochemistry 19*, 929–934.

Berliner, L. J., & Wong, S. S. (1975) *Biochemistry 14*, 4977–4982.

Berliner, L. J., & Kaptein, R. (1981) *Biochemistry 20*, 799–807.

[9] While it was experimentally difficult to accurately measure weak site binding dissociation constants by ESR Mn(II) displacement for other cations, a gradual but steady increase in free Mn(II) was noted in experiments similar to those in Figure 6 or 7 if one titrated well beyond the major binding curve. It is thus probable that up to three weak sites may exist for Ca(II) and other metals on bovine (and other) α-lactalbumins.

Berliner, L. J., Andree, P. J., & Kaptein, R. (1978) *Int. Conf. Magn. Reson. Biol. Syst., Nara, Japan, 7th*, 115.
Brittain, H. G., Richardson, F. S., & Martin, R. B. (1976) *J. Am. Chem. Soc. 98*, 8255-8260.
Dwek, R. A. (1973) *N.M.R. in Biochemistry*, Chapter 9, Clarendon Press, Oxford, England.
Hiraoka, Y., Segawa, T., Kuwajima, K., Sugai, S., & Murai, N. (1980) *Biochem. Biophys. Res. Commun. 95*, 1098-1104.
Kim, Y. S., & Padilla, G. M. (1978) *Anal. Biochem. 89*, 521-528.
Ley, J. M., & Jenness, R. (1970) *Arch. Biochem. Biophys. 138*, 404-414.
Permyakov, E. A., Yarmolenko, V. V., Kalinichenko, L. P., Morozova, L. A., & Burstein, E. A. (1981a) *Biochem. Biophys. Res. Commun. 100*, 191-197.
Permyakov, E. A., Kalinichenko, L. P., Morozova, L. A., Yarmolenko, V. V., & Burstein, E. A. (1981b) *Biochem. Biophys. Res. Commun. 102*, 1-7.
Prieels, J. P., Bell, J. E., Schindler, M., Castellino, F. J., & Hill, R. L. (1979) *Biochemistry 18*, 1771-1776.
Sommers, P. B., & Kronman, M. J. (1980) *Biophys. Chem. 11*, 217-232.
Warme, P. E., Momany, F. A., Romball, S. W., & Scheraga, H. A. (1974) *Biochemistry 13*, 768-781.

Factor Va-Factor Xa Interaction. Effects of Phospholipid Vesicles of Varying Composition†

Theo Lindhout,* José W. P. Govers-Riemslag, Piet van de Waart, H. Coenraad Hemker, and Jan Rosing

ABSTRACT: The interaction between factor Xa and factor Va was investigated both in solution and in the presence of phospholipid vesicles with varying contents of phosphatidylserine. The binding parameters were inferred from the kinetics of prothrombin activation. Factor Xa and factor Va form in solution an equimolar complex with a dissociation constant of 3.3×10^{-9} M. Phospholipid vesicles promote the formation of the factor Xa-Va complex. The K_d of complex formation is dependent on both the phospholipid concentration and the composition of the phospholipid vesicle. For the interaction between factor Xa and factor Va in the presence of phospholipid vesicles containing 40 mol % dioleoylphosphatidylserine (DOPS) and 60 mol % dioleoylphosphatidylcholine (DOPC), the K_d increases linearly with increasing phospholipid concentration. In the presence of 10 μM phospholipid (DOPS/DOPC, 40/60 mol/mol) $K_d = 3 \times 10^{-11}$ M. When the mole percentage of DOPS in the phospholipid vesicles is lowered from 20 to 5 mol %, there is a gradual increase of the K_d. In the presence of 10 μM phospholipid vesicles containing 5 mol % DOPS and 95 mol % DOPC $K_d = 2.8 \times 10^{-10}$ M. The K_d measured in the presence of phospholipid vesicles containing 5 mol % DOPS and 95 mol % DOPC is independent of the phospholipid concentration. Two models are discussed that can quantitatively explain the effect of phospholipid vesicles on the complex formation between factor Xa and factor Va. Studies on the effect of the polypeptides with M_r 80 000 and M_r 94 000 of which factor Va is composed on the K_d of the factor Xa-Va complex suggest that factor Xa binding to factor Va requires a Ca^{2+}-mediated interaction between the two polypeptides.

The activation of blood coagulation factor II (prothrombin)[1] into thrombin, catalyzed by the serine protease factor Xa, requires at physiological conditions the presence of the nonenzymatic components phospholipid, Ca^{2+} ions, and factor Va. It has been shown that these so-called accessory components augment the rate of prothrombin activation and that a prothrombinase complex composed of factor Xa, negatively charged phospholipid, Ca^{2+}, and factor Va is the most efficient in catalyzing prothrombin activation (Suttie & Jackson, 1977).

Kinetic studies on prothrombin activation by prothrombinase complexes of different composition (factor Xa in either the absence or presence of phospholipid, Ca^{2+}, and/or factor Va) reveal that phospholipids cause a profound decrease of the K_m for prothrombin, while factor Va causes a drastic increase of the V_{max} of thrombin formation (Rosing et al., 1980). The changes of the kinetic parameters caused by the accessory components are consistent with a model in which phospholipid provides a surface upon which factor Xa, factor Va, and prothrombin interact at increased local concentrations and factor Va changes the catalytic capacity of factor Xa.

Another important function of factor Va in haemostasis was discovered by Miletich et al. (1978). Their experiments suggest that factor Va is part of a highly specific factor Xa binding site on human blood platelets. The same tight binding site for factor Xa is also present at the surface of bovine blood platelets (Dahlbäck & Stenflo, 1978). Recently, Tracy et al. (1981) demonstrated that factor Xa and factor Va interact stoichiometrically at the platelet surface and that factor Xa binds to platelet-bound factor Va with an apparent dissociation constant of 6×10^{-10} M. Similar binding parameters were obtained in a phospholipid model system (Nesheim et al., 1979b).

The precise mode of action of phospholipid in promoting the interaction between factor Xa and factor Va is not known. In fact, it is not unequivocally demonstrated that factor Xa-Va complex formation at the platelet surface is the result of protein-phospholipid interaction per se. While Bevers et al.

† From the Department of Biochemistry, Biomedical Center, Rijksuniversiteit Limburg, Maastricht, The Netherlands. *Received March 12, 1982.* P.v.d.W. was supported by the Netherlands Organization for the Advancement of Pure Scientific Research (Z.W.O.).

[1] The nomenclature of the blood coagulation factors used is that recommended by the Task Force on Nomenclature of Blood Clotting Zymogens and Zymogen Intermediates.

0006-2960/82/0421-5494$01.25/0